Taylor & Francis
Taylor & Francis Group

Laser-induced fluorescence spectroscopy of $^{14}N^{18}O$ and its application to breath analysis

Christoph Mitscherling[a]*, Christof Maul[a], Alexei A. Veselov[b] and Karl-Heinz Gericke[a]

[a]*Institut für Physikalische und Theoretische Chemie, Technische Universität Braunschweig, Braunschweig, Germany;* [b]*Ioffe Physico-Technical Institute, St.Petersburg, Russian Federation*

Laser-induced fluorescence (LIF) spectroscopy is an efficient tool for the detection of low nitric oxide (NO) concentrations down to the parts per trillion (ppt) range. The isotopic selectivity of this method provides a broad potential of applications. Whereas $^{14}N^{16}O$ and $^{15}N^{16}O$ have been described extensively this is not the case for the $^{14}N^{18}O$ isotopologue. A (1+1) resonance enhanced multiphoton excitation time-of-flight mass spectrometer has been used for the simultaneous detection of $^{14}N^{16}O$, $^{15}N^{16}O$ and $^{14}N^{18}O$ isotopologues. Regions with single $^{14}N^{18}O$ transitions have been studied in more detail by the LIF device. Electronic excitation of the A-X transition in the UV provides fluorescence which is monitored around 247 nm from $A^2\Sigma^+(v'=0) \rightarrow X^2\Pi_\Omega(v''=2)$. This transition has been used for an isotope specific online detection of $^{14}N^{18}O$ from exhaled air. The detection limit for $^{14}N^{18}O$ is 7.3 ± 1.8 ppt. With respect to ^{18}O-labelled drugs and amino acids this denotes a novel extension to NO research.

Keywords: laser-induced fluorescence spectroscopy; $^{14}N^{18}O$; nitrogen-14; online breath analysis; oxygen-18

1. Introduction

Nitric oxide (NO) plays an important role in a multitude of processes in the atmosphere, mammalian physiology, plants, bacteria [1] and soils [2]. As a product of biomass and fuel combustion processes NO participates in the ozone formation of the lower troposphere and ozone depletion in the stratosphere [3]. In the human body it takes part in blood pressure regulation, immune defence, memory of the brain and many other processes [4, 5]. Plants utilise NO as a multifarious signal molecule in growth and differentiation processes [6–8]. Concentration measurement of exhaled NO is a well-established procedure for monitoring inflammatory diseases such as asthma [9, 10]. Commercial detection devices achieve detection limits of about 1 parts per billion (ppb), but are not able to differentiate between isotopologues. In contrast, we apply laser-induced fluorescence (LIF) spectroscopy which offers an isotope specific detection of NO with a time resolution of 20 ms and detection limits about 10 parts per trillion (ppt) [11]. The isotopic selectivity of this method has been used by Lauenstein and Gericke [12] for time resolved characteristics of exhaled

---

Table 1. Stable isotopologues of NO and natural distribution [13].

Isotopologue	Fraction %
$^{14}N^{16}O$	99.39288
$^{15}N^{16}O$	0.36912
$^{14}N^{18}O$	0.19926
$^{14}N^{17}O$	0.03786
$^{15}N^{18}O$	0.00074
$^{15}N^{17}O$	0.00014

$^{15}N^{16}O$ after oral intake of ^{15}N labelled L-Arginine, which is involved in NO production of the human body. The possibility to additionally detect the $^{14}N^{18}O$ isotopologue opens up new vistas for the time depending observation of metabolic processes through the application of ^{18}O labelled substances. Furthermore, ^{18}O-labelling will answer important questions concerning dynamics of NO transport as well as its storage and transformation within the living organism.

For the usage of isotope specific LIF experiments it is necessary to find spectral regions with transitions of one single isotopologue not interfering with others. Standard physiological NO samples consist of isotopologues due to the natural isotopic distribution. Under these conditions, the concentration of $^{14}N^{18}O$ is about the factor 500 smaller than that of the main compound $^{14}N^{16}O$. In order to find and observe individual $^{14}N^{18}O$ transitions it is essential to have knowledge of the line position because observation of the minor isotopologues is only possible under absence of strong $^{14}N^{16}O$ transitions. The search for these regions can be supported by simulation of NO spectra. Spectroscopic data for the $A^2\Sigma^+$ and $X^2\Pi_\Omega$ states of $^{14}N^{16}O$ and $^{15}N^{16}O$ have been measured and tabulated [14–16]. However, values for the excited $A^2\Sigma^+$ state of $^{14}N^{18}O$ from experimental data can not be found which makes a simulation less reliable. The calculation of the rotational constant B and the quartic centrifugal distortion D is possible but it is not for the spin-rotation-coupling constant γ and the band origin T_{00}. Therefore, we applied a (1+1) resonance enhanced multiphoton absorption (REMPI) setup combined with a time-of-flight (TOF) spectrometer to observe the three main isotopologues $^{14}N^{16}O$ ($M = 30$ u), $^{15}N^{16}O$ ($M = 31$ u) and $^{14}N^{18}O$ ($M = 32$ u) with different masses simultaneously. Interference with isotopologues of similar masses like $^{14}N^{17}O$ and $^{15}N^{17}O$ are small and can be neglected. Artificial and instable isotopes like ^{15}O, ^{13}N and ^{16}N have short lifetimes, thus, they are not important. Table 1 displays an overview of all stable isotopologues of NO and its natural fractions. The evaluation of REMPI measurements reveals some areas in the NO $\gamma(0,0)$-band system where detection of $^{14}N^{18}O$ transitions is possible and not interfering with transitions of other isotopologues. Subsequently, these areas have been studied with a LIF spectroscopy experiment. The LIF device is more flexible for the online investigation of biological samples with a theoretical detection limit for NO below 0.1 ppt [17]. The following chapter provides an overview of the REMPI TOF device and the additionally used LIF setup. Furthermore, the transitions have been used for the online observation of $^{14}N^{18}O$ in exhaled human air, and the detection limit for this isotopologue in LIF measurements has been determined.

2. Experimental section

A detailed description of the (1+1)-REMPI-TOF experimental setup can be found elsewhere [18]. The device consists of a home-built single-field TOF spectrometer with a total length of 0.57 m and a ratio of the acceleration region to the drift region of 1:2. The spectrometer is evacuated to a base pressure of 10^{-6} mbar by a 360 L/s turbo molecular pump and a 500 L/s oil diffusion pump.
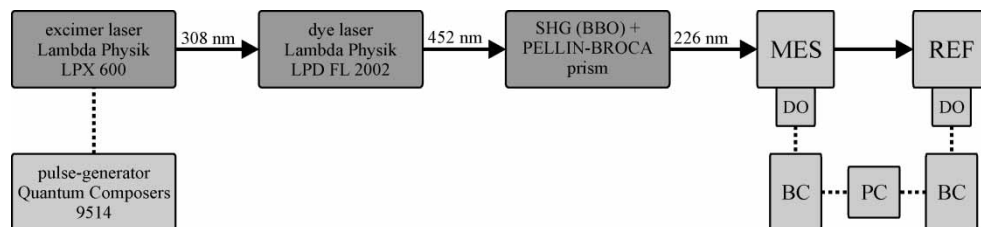
Figure 1. Brief overview of experimental LIF setup. SHG, second harmonic generation; MES, measuring cell; REF, reference cell; DO, detection optics and photomultiplier; BC, boxcar; PC, computer and multi-I/O-PC plug-in card.

Without further purification pure NO (2.5, Messer Griesheim GmbH) was fed into the spectrometer with a pressure of $5 \cdot 10^{-5}$ mbar. The $NO(X^2\Pi_{1/2})$ molecules were ionised by $(1+1)$ REMPI with usage of the $A^2\Sigma^+$ state as a resonant intermediate. This was achieved by using a dye laser pumped by an externally triggered (Quantum Composers 9514) excimer laser (Lambda Physik LPX 600). The dye laser (Lambda Physik FL 2002) is operated with Coumarin 47 at repetition rates of 10 Hz. A consecutive β-barium borate crystal provides wavelengths around 226 nm which are separated from the first harmonic by a unit of four PELLIN-BROCA prisms. The multichannel plate (MCP) (in Chevron arrangement) signal of the TOF spectrometer was processed by three boxcar integrators (SR 250), optically triggered by a scattered light detecting photodiode in the dye laser. Each of the three boxcar integrators was gated on the NO isotopologue signal of interest. The output signal is fed into an analogue/digital converter and then to a multi-I/O-PC plug-in card. A LabVIEW program (National Instruments Corporation) recorded the data.

The LIF device was operated with the same laser system as mentioned above for the REMPI experiments. Separation of the first and second harmonic is accomplished by a single PELLIN-BROCA prism. A detailed description of the experimental setup can be found in [11], a brief overview over the experimental LIF setup is given in Figure 1. We excite the $A^2\Sigma^+(v' = 0, J') \leftarrow X^2\Pi_{1/2}(v'' = 0, J'')$ around 226 nm. The beam is directed to a LIF chamber with BREWSTER windows. The f1 detection optic collects NO fluorescence from $A^2\Sigma^+(v' = 0, J') \rightarrow X^2\Pi_\Omega(v'' = 2, J'')$ around 247 nm perpendicular to the incoming beam and focuses it on a side-on photomultiplier (PM) (Hamamatsu R3788). The fluorescence is spectrally filtered by a bandpass filter (Andover Corporation 248FS10-50). The PM signal is processed by a boxcar with 50Ω input resistance and recorded by a LabVIEW program after analogue/digital conversion.

The mass-flux system for the chamber is able to provide online measurements of arbitrary air samples. It consists of two mass flow controllers (MKS Instruments 1179A) operated by a control unit (MKS Instruments PR4000) and a pressure controller (MKS Instruments 250E) for dynamic mass flows employing a capacity pressure gauge head (MKS Instruments Baratron 221 AHS-D-100) and an electromagnetic valve (MKS Instruments 248A). The valve and an optional bypass for handling larger mass flows are connected to a piston pump (Pfeiffer Vakuum XtraDry 150-2). A home-built breath mask with a nitrogen-rinsing device can be applied for monitoring breath profiles of exhaled air.

3. Results and discussion

The REMPI experiments have been performed with pure NO at pressures about $5 \cdot 10^{-5}$ mbar. For the MCP an operational voltage of 2 kV has been applied and for the TOF acceleration region a 10^4 V/m acceleration field. Each isotopologue has been gated by a single boxcar. Because of the significant concentration difference between $^{14}N^{16}O$ and $^{15}N^{16}O/^{14}N^{18}O$ (see Table 1) the former signals are much stronger and therefore overlap with the $^{15}N^{16}O/^{14}N^{18}O$ boxcar-gates. Only in the

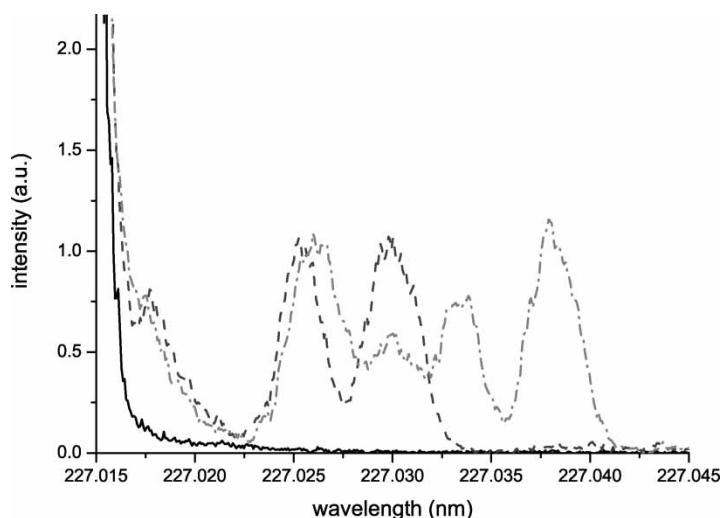Figure 2. (1+1)-REMPI TOF spectrum from 227.015 to 227.045 nm for the three main isotopologues of NO. — $^{14}N^{16}O$; − − − $^{15}N^{16}O$; · − ·− $^{14}N^{18}O$.

absence of any $^{14}N^{16}O$ transition $^{15}N^{16}O$ and $^{14}N^{18}O$ can be observed separately. We measured the NO spectra with REMPI in 0.4 nm intervals in the region between 225.7 and 226.8 nm (0.5 pm resolution). Two regions of interest are shown in Figures 2 and 3. $^{14}N^{18}O$ signals in light grey are clearly distinguishable from the other isotopologues. These signal peaks are available for interference-free concentration determination of $^{14}N^{18}O$.

These regions with single $^{14}N^{18}O$ transitions have been observed further by LIF spectroscopy. The measuring chamber was filled with 2.5 ppm NO in N_2 (certified 2.5 vol. ppm NO in N_2, Westfalen AG, uncertainty 5%) at 12 mbar. With PM voltages of 1400 V we measured in detail three regions with a resolution of 0.5 pm. Each region has been measured 10 times. After averaging and fitting of multiple Gaussian curves, the result has been compared to simulated spectra. Figures 4–6
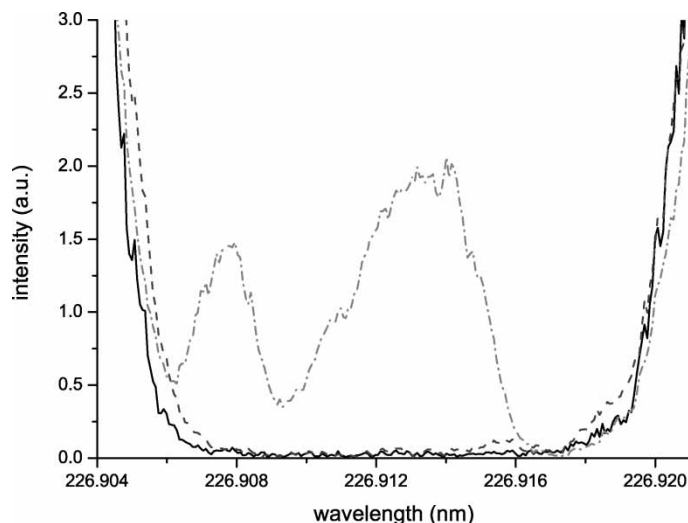

Figure 3. (1+1)-REMPI TOF spectrum from 226.904 to 226.921 nm for the three main isotopologues of NO. — $^{14}N^{16}O$; − − − $^{15}N^{16}O$; · − ·− $^{14}N^{18}O$.

show the measured and calculated spectra. All lines can be assigned. The simulation has been performed by the program Pgopher [19]. A list of constants for simulation is given in Table 2. B and D from the $^{14}N^{18}O$ $A^2\Sigma^+$-state have been calculated whereas γ and T_{00} are fitted parameters. B is a function of the moment of inertia I due to

$$B = \frac{h}{8 \cdot \pi^2 \cdot I \cdot c} \tag{1}$$

with

$$I = \mu \cdot R^2 \tag{2}$$

c as the speed of light in vacuum and h as the Planck constant. The I value is a function of the reduced mass μ of the isotopologue and the intermolecular distance R. The assumption of equal R for different isotopologues 1 and 2 yields

$$\frac{B_1}{B_2} = \frac{I_2}{I_1} = \frac{\mu_2}{\mu_1} \tag{3}$$

Calculation of the ground-state $^2\Pi_\Omega$ B-value for $^{14}N^{18}O$ from $^{14}N^{16}O$-data with $\mu_{^{14}N^{16}O} = 7.466433$ and $\mu_{^{14}N^{18}O} = 7.875812$ results in a ratio $I_{^{14}N^{16}O}/I_{^{14}N^{18}O} = 0.948021$. According to this $B_{\Pi,^{14}N^{18}O} = 1.60791\,\mathrm{cm}^{-1}$, which is in good agreement with the experimental data [20]. Under the same assumptions, the corresponding B values for the excited $^2\Sigma$ state have been calculated from known constants of $^{14}N^{16}O$. For the following experiments, we employed a distinct $^{14}N^{18}O$ signal for isotopologue selective observation. The strongest $^{14}N^{18}O$ signal, not disturbed by other isotopologues, is the combination of $^PQ_{12}(2.5) + {^P}P_{22}(2.5) + {^P}Q_{12}(3.5) + {^P}P_{22}(3.5)$ at about 226.9144 nm with $^{\Delta N}\Delta J_{F'F''}(J'')$. While detecting the fluorescence, a dynamic mass flux is diluted stepwise for the determination of the detection limit. This is done by a mass flow controller adjusted mixture of nitrogen and 2.5 ppm NO in nitrogen mass fluxes. The detection limit is characterised by a fluorescence signal-to-noise ratio of 2 at 7.3 ± 1.8 ppt. The calculation of the $^{14}N^{18}O$ concentration from the 2.5 ppm NO mixture has been accomplished under assumption of

Figure 4. LIF spectrum of 2.5 ppm NO in N_2 from 226.374 to 226.402 nm. The dotted black line is an average over 10 measurements. — simulation of $^{14}N^{16}O$; – – – simulation of $^{15}N^{16}O$; · – ·– simulation of $^{14}N^{18}O$.
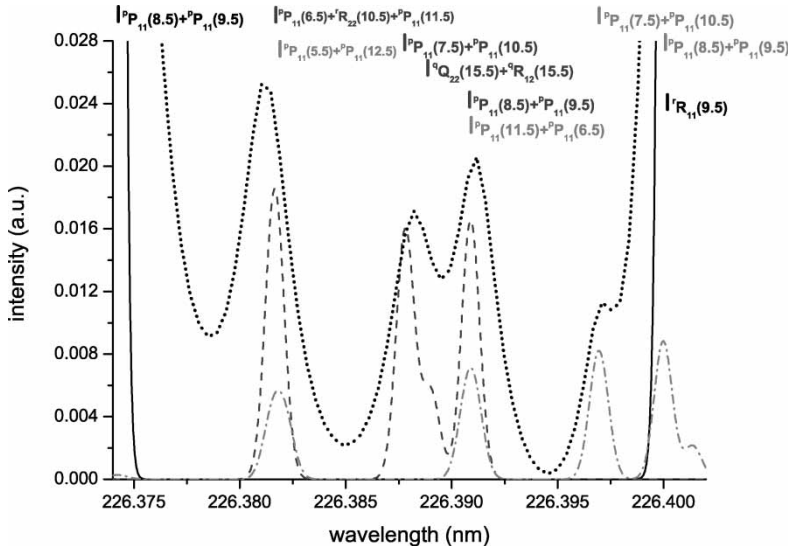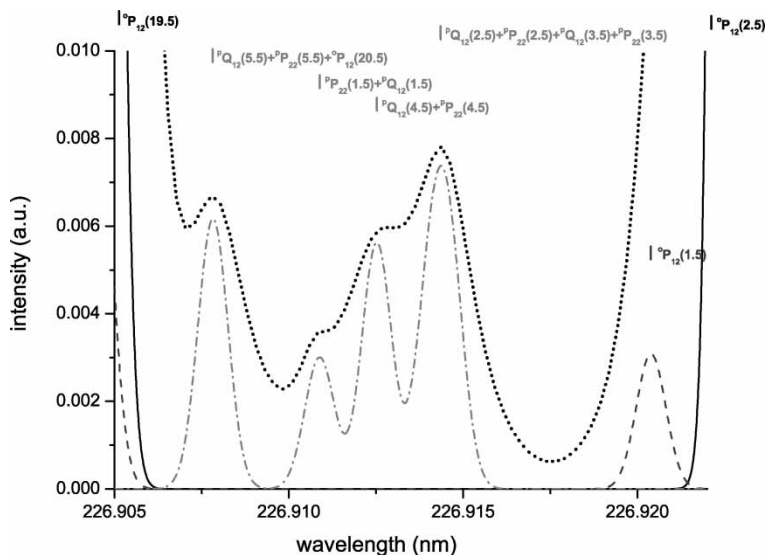
Figure 5. LIF spectrum of 2.5 ppm NO in N_2 from 226.905 to 226.922 nm. The dotted black line is an average over 10 measurements. — simulation of $^{14}N^{16}O$; − − − simulation of $^{15}N^{16}O$; · − ·— simulation of $^{14}N^{18}O$.

natural isotopic distribution. This has been circumstantiated by strength comparison of identical transitions for different isotopologues giving the ratios of natural distribution.

As an application for $^{14}N^{18}O$ detection the well-established breath analysis has been chosen. Exhaled air contains about 1200 compounds and trace gases [21]. Especially with respect to isotope-selective detection in online breath measurements cross-sensitivities should be excluded. The laser-line width of the applied device is about 15 GHz which is sufficient for the resolution of nearby transitions from different isotopologues. Because of very low concentrations from both, NO and trace-gases, reactions reducing the NO concentration as well as photochemical generation
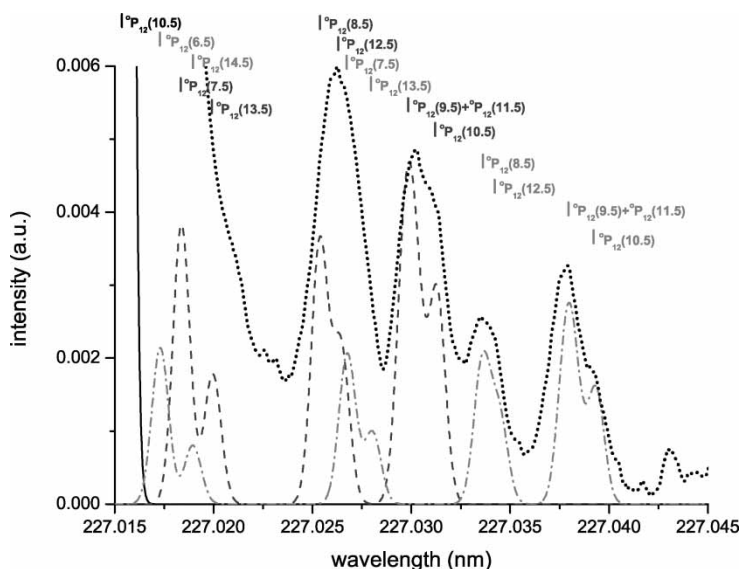

Figure 6. LIF spectrum of 2.5 ppm NO in N_2 from 227.015 to 227.045 nm. The dotted black line is an average over 10 measurements. — simulation of $^{14}N^{16}O$; − − − simulation of $^{15}N^{16}O$; · − ·— simulation of $^{14}N^{18}O$.

Table 2. Constants for simulation of $\gamma(0, 0)$ NO spectra in cm^{-1}.

| | $^{14}N^{16}O$ | | $^{15}N^{16}O$ | | $^{14}N^{18}O$ | |
	$X^2\Pi_\Omega$	$A^2\Sigma^+$	$X^2\Pi_\Omega$	$A^2\Sigma^+$	$X^2\Pi_\Omega$	$A^2\Sigma^+$
T_{00}	–	44139.128[b]	–	44134.864	–	44132.860
B	1.69607[a]	1.98622[a]	1.63616[a]	1.91603[a]	1.60817[c]	1.88320
A	123.14[a]	–	123.14[a]	–	123.14[c]	–
$\gamma \cdot 10^3$	–0.01489	–2.68[a]	–0.01572	–2.585[a]	–	–2.54[d]
$D \cdot 10^6$	5.472[a]	5.656[a]	5.092[a]	5.172[a]	4.924[c]	5.362[d]
$p \cdot 10^2$	1.17[a]	–	1.127[a]	–	1.108[c]	–
$q \cdot 10^5$	10.28[a]	–	8.917[a]	–	8.399[c]	–
$A_D \cdot 10^4$	1.792[a]	–	1.698[a]	–	1.650[c]	–

References: [a][14], [b][15], [c][20], [d]this work.

of NO are negligible. The measured spectra are in excellent agreement with the calculated ones showing that there is no fluorescence from other trace gases.

A detailed description of the device for breath analysis has been given before [11]. The respiration-mask is used for a non-invasive online observation of exhaled air. With mass fluxes about 1200 sccm per minute the measuring chamber is rinsed with nitrogen during inhalation periods. With a maximum resolution of 20 ms it is possible to observe both single exhalation profiles and long time profile evolution. A section from these measurements is shown in Figure 7 in grey. A laser pulse repetition rate of 10 Hz has been applied. The boxcar averaging was set to 3 laser-shots. An average of 30 laser-shots has been applied for the black line. Beginning (<80 s) and end (>350 s) of this experimental run reflects noise from pure nitrogen measurements. Absolute concentrations are given by application of the standard addition method on exhaled air in collection bags and by comparison with the signal integral of a single exhalation cycle [11]. The averaged concentration of exhaled $^{14}N^{18}O$ from the test person is 33 ± 4 ppt.

Averaging over more laser-shots would decrease the temporal resolution further. The maximum exhaled NO content varies from person to person. For a more general statement concerning the averaged exhaled $^{14}N^{18}O$ output more test persons have to be considered for an average

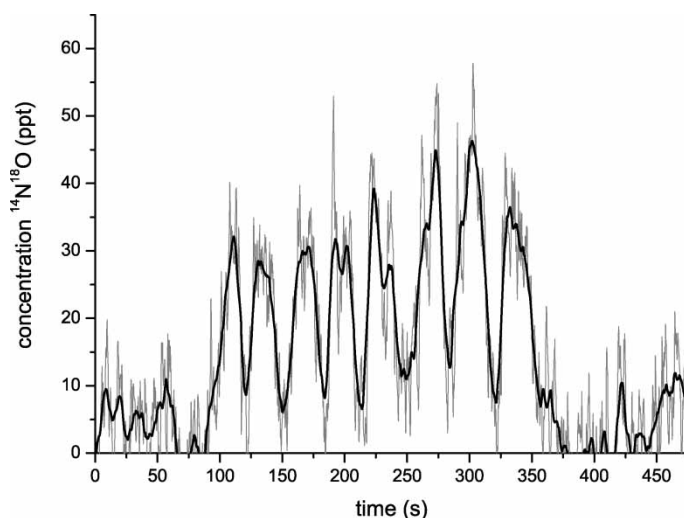Figure 7. Online breath measurement of exhaled $^{14}N^{18}O$. The grey line is a boxcar average over three laser shots. The black line is an average over 30 points.

sample. Considering the natural isotopic distribution the overall exhaled NO concentration of the test person is 17 ppb. Because of quenching gases in exhaled air which reduce the observable fluorescence the detection limit can vary between different individuals.

4. Conclusions

With a (1+1) REMPI experiment we are able to observe different isotopologues of NO separately. Because a simulation of a $^{14}N^{18}O$ UV spectrum of the γ-band is not reliable these REMPI measurements have been applied to reveal regions for isotope-selective detection of $^{14}N^{18}O$. These regions have been observed further with a LIF device. The $^{14}N^{18}O$ spectra have been fitted by simulated spectra and unknown constants for the excited $A^2\Sigma^+$ state have been estimated. To our knowledge, the strongest signal of $^pQ_{12}(2.5) + {}^pP_{22}(2.5) + {}^pQ_{12}(3.5) + {}^pP_{22}(3.5)$ at about 226.9144 nm has been used for the first time for an online detection of $^{14}N^{18}O$ in exhaled air. The detection limit for this isotopologue is 7.3 ± 1.8 ppt and the maximum time-resolution 20 ms. Usage of laser systems with higher repetition rates will provide even better time-resolutions.

This method offers an additional possibility for the application of isotopes in chemical, medical and biological research because NO is an important biomarker. Beside the earlier described usage of $^{15}N^{16}O$ for time resolved metabolism investigation we demonstrate the possibility of applying ^{18}O labelled drugs or amino acids in NO related research.

References

[1] H. Corker and R.K. Poole, Nitric Oxide Formation by *Escherichia coli*, *J. Biol. Chem.* **278**(34), 31584–31592 (2003).
[2] K.H. Cho and J.J. Peirce, Nitric Oxide Emissions from Soils to Lower Levels of the Troposphere, *Environ. Eng. Sci.* **22**(1), 46–57 (2005).
[3] R. Delmas, D. Serca and C. Jambert, Global Inventory of NO_x Sources, *Nutr. Cycling Agroecosyst.* **48**, 51–60 (1997).
[4] G. Knowles and S. Moncada, Nitric Oxide Synthases in Mammals, *Biochem. J.* **298**, 249–258 (1994).
[5] S. Moncada, R.M. Palmer and E.A. Higgs, Nitric Oxide: Physiology, Pathophysiology and Pharmacology, *Pharmacol. Rev.* **43**, 109–136 (1991).
[6] L. Lamattina, C. Garcia-Mata, M. Graziano and G. Pagnussat, Nitric Oxide: The Versatility of an Extensive Signal Molecule, *Annu. Rev. Plant Biol.* **54**, 109–136 (2003).
[7] L.A. del Rio, F.J. Corpas and J.B. Barroso, Nitric Oxide and Nitric Oxide Synthase Activity in Plants, *Phytochemistry* **65**, 783–792 (2004).
[8] E. Planchet and W.M. Kaiser, Nitric Oxide Production in Plants, *Plant Signal. Behav.* **1**(2), 46–51 (2006).
[9] American Thoracic Society Documents, ATS/ERS Recommendations for Standardized Procedures for the Online and Offline Measurement of Exhaled Lower Respiratory Nitric Oxide and Nasal Niric Oxide, *Am. J. Respir. Crit. Care Med.* **171**, 912–930 (2005).
[10] S.A. Kharitonov and P.J. Barnes, Clinical Aspects of Exhaled Nitric Oxide, *Eur. Respir. J.* **16**, 781–792 (2000).
[11] C. Mitscherling, J. Lauenstein, C. Maul, A.A. Veselov, O.S. Vasyutinskii and K.-H. Gericke, Non-Invasive and Isotope-Selective Laser-Induced Fluorescence Spectroscopy of Nitric Oxide in Exhaled Air, *J. Breath Res.* **1**, 9 (2007).
[12] J. Lauenstein and K.-H. Gericke, in *Breath Analysis for Clinical Diagnosis and Therapeutic Monitoring, Chapter B: Isotope Selective Detection of Nitric Oxide in Human Exhalation*, edited by A. Amann and D. Smith (World Scientific, New Jersey, 2005), pp.161–169.
[13] <http://physics.nist.gov/PhysRefData/Elements/index.html, 05 2007>.
[14] J. Danielak, U. Domin, R. Kępa, M. Rytel and M. Zachwieja, Reinvestigation of the Emission Band System ($A^2\Sigma^+ - X^2\Pi$) of the NO Molecule, *J. Mol. Spectr.* **181**, 394–402, (1997).
[15] R. Freedman and R.W. Nicholls, Notes: Molecular Constants for the $v'' = 0(X^2\Pi)$ and $v' = 0, 1$ $(A^2\Sigma^+)$ Levels of the NO Molecule and Its Isotopes, *J. Mol. Spectr.* **83**, 223–227, (1980).
[16] S.P. Reddy and C. Haridass, in *Ultraviolet Spectroscopy and UV-Lasers, Chapter 3: Spectra of the Isotopomers of CO^+, N_2^+, and NO in the Ultraviolet*, edited by P. Misra and M.A. Dubinskii (Marcel Dekker Inc, Ney York, 2002), pp.106–120.
[17] J. Lauenstein, Isotopenselektiver Nachweis von biologisch freigesetztem Stickstoffmonoxid, Ph.D. dissertation, Technische Universität Braunschweig, 2006.

[18] T. Haas, C. Maul and K.-H. Gericke, Photodissociation Dynamics of HN_3. The N_3 Fragment Internal Energy Distribution, *Chem. Phys. Lett.* **202**(1,2), 108–114, (1993).

[19] C.M. Western, Pgopher, a Program for Simulating Rotational Structure, <http://pgopher.chm.bris.ac.uk/>, University of Bristol.

[20] E. Klisch, S.P. Belov, R. Schieder, G. Winnewisser and E. Herbst, Transitions Between Hund's Coupling Case for the $X^2\Pi$ State of NO, *Mol. Phys.* **97**(1,2), 65–79 (1999).

[21] M. Philips, Method for the Collection and Assay of Volatile Organic Compounds in Breath, *Analyt. Biochem.* **247**(2), 272–278, (1997).